HHS Public Access

Author manuscript

Neurochem Int. Author manuscript; available in PMC 2024 April 03.

Published in final edited form as:

Neurochem Int. 2023 June ; 166: 105524. doi:10.1016/j.neuint.2023.105524.

A role for protein arginine methyltransferase 7 in repetitive and mild traumatic brain injury

Christina H. Acosta[a], **Garrett A. Clemons**[a], **Cristiane T. Citadin**[a], **William C. Carr**[b], **Mariana Sayuri Berto Udo**[b], **Vesna Tesic**[b], **Henry W. Sanicola**[b,c], **Anne H. Freelin**[c], **Jamie B. Toms**[c], **J. Dedrick Jordan**[b], **Bharat Guthikonda**[c], **Celeste Yin-Chieh Wu**[b], **Reggie Hui-Chao Lee**[b], **Hung Wen Lin**[a,b,*]

[a]Department of Cellular Biology & Anatomy, Louisiana State University Health Sciences Center, Shreveport, LA, USA

[b]Department of Neurology, Louisiana State University Health Sciences Center, Shreveport, LA, USA

[c]Department of Neurosurgery, Louisiana State University Health Sciences Center, Shreveport, LA, USA

Abstract

Mild traumatic brain injury affects the largest proportion of individuals in the United States and world-wide. Preclinical studies of repetitive and mild traumatic brain injury (rmTBI) have been limited in their ability to recapitulate human pathology (i.e. diffuse rotational injury). We used the closed-head impact model of engineered rotation acceleration (CHIMERA) to simulate rotational injury observed in patients and to study the pathological outcomes post-rmTBI using C57BL/6J mice. Enhanced cytokine production was observed in both the cortex and hippocampus to suggest neuroinflammation. Furthermore, microglia were assessed via enhanced iba1 protein levels and morphological changes using immunofluorescence. In addition, LC/MS analyses revealed excess glutamate production, as well as diffuse axonal injury via Bielschowsky's silver stain kit. Moreover, the heterogeneous nature of rmTBI has made it challenging to identify drug therapies that address rmTBI, therefore we sought to identify novel targets in the concurrent rmTBI pathology. The pathophysiological findings correlated with a time-dependent decrease in protein arginine methyltransferase 7 (PRMT7) protein expression and activity post-rmTBI along with dysregulation of PRMT upstream mediators s-adenosylmethionine and methionine

*Corresponding author. Department of Neurology, LSU Health Sciences Center Shreveport, 1501 Kings Hwy, Shreveport, LA, 71103-3932, USA. hungwen.lin@lsuhs.edu (H.W. Lin).

Author contributions

Christina H. Acosta performed the experiments, wrote the manuscript, and provided scientific input. Garrett A. Clemons provided scientific input and assisted in analysis and quantification. Cristiane T. Citadin assisted in designing real-time qPCR experiments. William C. Carr provided technical support and assisted in protein analysis. Mariana Sayuri Berto-Udo and Vesna Tesic assisted in manuscript preparation and editing. Henry W. Sanicola, Anne H. Freelin, Jamie B. Toms, Joseph D. Jordan, Bharat Guthikonda, Celeste Yin-Chieh Wu, Reggie Hui-Chao Lee, contributed scientific input to the manuscript. Hung Wen Lin provided scientific input, guidance, funding, and assisted in the composition of the manuscript.

Declaration of competing interest

The authors declare no conflict of interest.

Appendix A. Supplementary data

Supplementary data to this article can be found online at https://doi.org/10.1016/j.neuint.2023.105524.

adenosyltransferase 2 (MAT2) *in vivo*. In addition, inhibition of the upstream mediator MAT2A using the HT22 hippocampal neuronal cell line suggest a mechanistic role for PRMT7 via MAT2A *in vitro*. Collectively, we have identified PRMT7 as a novel target in rmTBI pathology *in vivo* and a mechanistic link between PRMT7 and upstream mediator MAT2A *in vitro*.

Keywords

Protein arginine methyltransferase; Methionine adenosyltransferase 2; Traumatic brain injury; PF-9366; S-adenosylmethionine

1. Introduction

Traumatic brain injury (TBI) is a leading cause of death and disability world-wide for individuals 45 years of age and under and contributes to a global economic burden of ~$400 billion USD annually (Namjoshi et al., 2014; Maas et al., 2017). TBI is caused by an external force such as a jolt, blow, or blunt penetrating trauma that can cause brain tissue deformation and subsequent behavioral, locomotor, and cognitive alterations (Namjoshi et al., 2014; Ginsburg and Huff, 2022; McKee and Daneshvar, 2015; Bodnar et al., 2019). The severity of TBI can vary from mild to severe depending on the location of the impact, object penetration, age, sex, and number of repetitive head injuries incurred throughout life (Namjoshi et al., 2014; McKee and Daneshvar, 2015). Repetitive and mild TBI (rmTBI) accounts for an estimated 82.3 % of all TBI-related traumas leading to long-term cognitive impairment and emotional distress (McKee and Daneshvar, 2015; Namjoshi et al., 2014).

Post-injury, TBI events are categorized into primary (caused by the initial impact) and secondary injury (consequences of the primary injury that can last for days, weeks, months, and years) (McKee and Daneshvar, 2015). In addition, TBI contributes to innumerable biochemical and physiological changes such as: neuroinflammation, diffused axonal injury (DAI), glutamate induced excitotoxicity, oxidative stress, mitochondrial dysfunction, blood-brain-barrier (BBB) permeability, impaired cerebral blood flow, and ischemic/hypoxic damage (McKee and Daneshvar, 2015). For our rmTBI studies, we used the closed-head impact model of engineered rotational acceleration or CHIMERA as it is a (non-surgical) clinically relevant model of TBI that allows free head rotation upon impact generated from a compressed air-driven piston (Namjoshi et al., 2014). Prior research models (i.e open head controlled cortical impact, fluid percussion injury, weight drop model etc.) of TBI lack the clinical relevance of rotational injury seen in patients that are involved in automobile accidents, falls, and high impact sports. In addition, this model allows for high-throughput workflow, as it does not require surgery or use of analgesics (Namjoshi et al., 2014).

The heterogeneous nature of rmTBI has made it challenging to identify drug therapies as there is no single therapeutic that can mitigate the myriad of symptoms that arise from rmTBI. Due to this limitation along with very few FDA approved biomarkers/targets to diagnose TBI, we sought to identify novel targets in the disease pathology in our *in vivo* model of rmTBI. Novel therapeutic targets include protein arginine methyltransferases (PRMTs), which are enzymes responsible for methylating arginine residues located on histones and non-histone target proteins (Couto et al., 2020). The PRMT family consists of

enzymes (PRMT1-11) and are classified as Type I, II, or III depending on their end-product formation. Type I PRMTs (PRMT1-4, 6, 8) methylate L-arginine to produce asymmetric dimethylarginine (ADMA), Type II (PRMT5, 9) produce symmetric dimethylarginine (SDMA) and type III PRMT (PRMT7) produces mono-methylarginine (MMA) as its' end-product (Couto et al., 2020; Jain and Clarke, 2019). PRMT7 is of particular interest as it is the only type III PRMT (producing MMA as its' end-product) (Couto et al., 2020; Jain and Clarke, 2019) and human deletion of this gene has been implicated in intellectual disability, microcephaly, and brachydactyly (Kernohan et al., 2017; Valenzuela et al., 2019; Rodari et al., 2022; Cali et al., 2022). Moreover, PRMT7 has been implicated in neurological function via methylation of hyperpolarization-activated cyclic nucleotide-gated and sodium leak channels affecting neurotransmission within pyramidal cells of mouse hippocampi; to suggest an essential role for PRMT7 to maintain neuronal viability (Lee et al., 2020; Lee et al., 2019).

Methionine adenosyltransferase 2 (MAT2A) is responsible for s-adenosylmethionine (SAM) production, the universal methyl donor in the body, via the combination of ATP and L-methionine (C. Li et al., 2022). MAT2A and SAM are upstream mediators of PRMT activity as PRMT's utilize SAM to methylate their downstream substrates (Kalev et al., 2021). MAT2A is the extrahepatic form of this enzyme and exists as a homodimer (Nordgren et al., 2011), whereas MAT2B is the regulatory subunit and has been reported to regulate and inhibit MAT2A activity (Quinlan et al., 2017). Dysregulation of MAT enzymes have been shown to contribute to various forms of cancer including, but not limited to, liver, gastric, leukemia, and brain tumor proliferation (C. Li et al., 2022; Maldonado et al., 2018); moreover, methionine dysregulation has also been implicated in clinical studies of TBI (Dash et al., 2016).

Our rmTBI paradigm showed similar pathologies from previous studies such as neuroinflammation, enhanced microglia, excess glutamate, and diffuse axonal injury (Namjoshi et al., 2014; Xiong et al., 2018; Schwulst et al., 2013; Drieu et al., 2022; Tasker, 2012; McNamara et al., 2020). Furthermore, our aim was to identify concurrent potential therapeutic targets *in vivo*. Due to the clinical relevance and implication in neurological function, we sought to investigate a potential role for the PRMT7 enzyme in our model of rmTBI using C57BL/6 mice as well as to determine a mechanistic link between PRMT7 and upstream mediators MAT2A/B *in vitro* using HT22 hippocampal neuronal cell line.

2. Materials & Methods

2.1. Animal preparation

All experimental procedures were approved by the Institutional Animal Care and Use Committee of the Louisiana State University (LSU) Health Sciences Center Shreveport, LA. C57BL/6J male mice were purchased from Jackson Laboratory at 7 weeks old. Mice ages 8–12 weeks, weighing 20–32 g were used for all experiments. Mice were held in standard LSU Health Veterinary conditions with controlled air, humidity, and a 12 hr light to dark cycle. Upon completion of rmTBI experimentation, mice were placed into an induction chamber at (5 % isoflurane with 900 cc of O_2). Paw reflex was used as an indicator of a complete anesthetized mouse. The mice were then decapitated, and the brain (cortex

and hippocampus) harvested for subsequent assays. Mice were randomly placed into the following experimental groups: (SHAM/Control), 1, 3, 7-day endpoints, to assess loss of righting reflex and molecular changes *in vivo*.

2.2. Loss of righting reflex (LRR)

Loss of righting reflex (LRR) indicates loss of consciousness in mice (Namjoshi et al., 2014). Mice were anesthetized and placed onto the CHIMERA TBI device (Namjoshi et al., 2014) after 2 min of induction with isoflurane (5 % isoflurane with 900 cc of O_2). Velcro straps were placed across the abdomen and chest to secure the mouse. An air-actuated piston was used to strike the back of the mouse head (where the bregma and lambda suture) allowing free rotation at 0.7 J for three consecutive hits (24 hrs apart) to induce rmTBI, which produced a loss of consciousness of the mouse. Elapsed time after each hit was measured by placing the mouse laterally in a mouse cage on top of a 37 °C heating pad to allow for proper recovery. Each mouse rolled over to the prone position after gaining consciousness with all 4 paws on the heating pad known as righting time. The elapsed time of 15 min or less indicates mild TBI in rodents (Sauerbeck et al., 2018; Dewitt et al., 2013).

2.3. Capillary-based immunoassay via ProteinSimple®

Capillary electrophoresis immunoassay, or Simple Western analyses, were performed using the Wes/Jess™, according to the manufacturer's protocol (ProteinSimple, Bio-techne, Minneapolis, MN). Protein isolation from the cerebral cortex and hippocampus was performed using T-PER® Tissue Protein Extraction Reagent (Cat. No. 78510, Thermo Fisher Scientific, Waltham, MA) with Halt™ Protease Inhibitor Cocktail (Cat. No. 87785, Thermo Fisher Scientific, Waltham, MA). Tissue lysates were diluted in sample buffer (Protein Simple®) to achieve a final concentration of 1 μg/μl and added to a master mix containing 40 mM fluorescent molecular weight marker with dithiothreitol (DTT). Samples were denatured at 95 °C for 5 min before loading into a 25 or 13-well plate and capillary cartridge with a target protein size of 12–230 kDa (Cat. No. SM-W001; ProteinSimple). All antibodies were diluted using an antibody diluent (ProteinSimple, Bio-techne, Minneapolis, MN) as follows: iba1 (1:50; GeneTex GTX100042), PRMT7 (1:100; D1K6R), Monomethylarginine (MMA 1:50; 8015S), (Cell Signaling Technology, Danvers, MA), Bax (1:50; R&D Systems AF820), MAT2A (1:500; Novus NB110-94158), MAT2B (1:40; ProteinTech 15952-I-AP). Antibody targets were detected with an HRP-conjugated secondary anti-rabbit or anti-mouse. Protein levels were calculated by the area under the curve from chemiluminescence chromatograms obtained via the Compass for SW software (version 4.0.0, Protein Simple, Bio-techne, Minneapolis, MN). Relative protein expression was calculated by protein peak intensity divided by the total protein loading control provided by the manufacturer. Compass for SW software-generated pseudo-blots are presented with each protein of interest (ProteinSimple®, Bio-techne, Minneapolis, MN).

2.4. Real-time quantitative reverse transcription polymerase chain reaction (RT-qPCR)

Mouse hippocampus and cortex were harvested and homogenized. mRNA was extracted using the QIAGEN RNeasy Mini Kit (Cat. No. 74104, QIAGEN, Hilden, Germany); with analyses of mRNA quality and quantity using the NanoDrop (Thermo Fisher Scientific, Waltham, MA). cDNA was synthesized from 500 ng of extracted mRNA with

Superscript™ III Reverse Transcriptase (Cat. No. 18080051, Thermo Fisher Scientific, Waltham, MA) according to the manufacturer's recommendations in a T100™ Thermal Cycler (BioRad, Hercules, CA). qPCR was performed in a CFX96 Real-Time PCR Detection System using iQ™ SYBR® Green Supermix (Cat. No. 1708886, Bio-Rad, Hercules, CA). The PCR reaction consisted of the following constituents: 0.4 μl of cDNA, 10 μl of iQ™ SYBR® Green Supermix (Invitrogen, Carlsbad, CA), 200 nM of each primer, and nuclease free water. The cycling conditions for the qPCR amplification were as follows: 95 °C for 3 min, 95 °C for 10 s, 60 °C for 30 s, for 40 cycles. Target genes were normalized with the housekeeping genes β-actin (forward 5′-AGCCATGTACGTAGCCATCC-3′ and reverse 5′-CTCTCAGCTGTGGTGGTGAA-3′) or GAPDH (forward 5′-CATCACTGCCACCCAGAAGACTG-3′ and reverse 5′-ATGCCAGTGAGCTTCCCGTTCAG-3′) (Narayan & Kumar, 2012). The mouse primer sequence for PRMT7 gene was obtained from Primer Bank (ID 21703807c1) database and synthesized by MilliporeSigma (MilliporeSigma, Burlington, MA) (forward 5′-TTGCCAGGTCATCCTATGCC-' and reverse 5′-GCCAATGTCAAGAACCAAGGC-3′).

2.5. Cytokine array

Mouse inflammation array (RayBiotech; QAM-INF-1-1) was used to detect the level of cytokines present in murine tissue lysates. This ELISA based analysis allowed for the quantification of the following cytokines: ICAM-1, IL-6, CD30-L, IL-5, IL-10, IL-1a, and IL-12p70, via a fluorescence laser scanner. Procedures were accordance to RayBiotech protocols and significant results were presented from the cortex and hippocampus. For further details, see our previous publication (Couto et al., 2021).

2.6. Histology (immunofluorescence)

Mice were anesthetized and transcardially perfused with 1 X phosphate buffered saline (PBS), followed by 4 % paraformaldehyde (Cat. No. P6148, MilliporeSigma, Burlington, MA) in 0.1 mmol/L of PBS. Brains were fixed in 4 % paraformaldehyde overnight at 4 °C, followed by dehydration in 30 % sucrose in 0.1 mmol/L PBS for 72 hrs at 4 °C before sectioning. Tissue was sectioned into 30 μm slices on a sliding microtome stage chilled to —20 °C (Leica Biosystems, SM2000R) in NEG-50™ sectioning media (Cat. No. 6502, Thermo Fisher Scientific, Waltham, MA, USA), and placed in a 24-well dish in 1 X PBS. Tissue slices were mounted on adhesion slides (Cat. No. M1000W, StatLab, McKinney, TX) and submerged into 1 X PBS with 0.1 % Triton (Sigma) rinsed thrice. Slides were placed into a humidity chamber (M918-2; Simport Scientific Inc.) and blocked with 1 % BSA, 0.1%, TritonX-100 in PBS for 1-hr incubation, followed by 3 × 15 min rinses. Primary antibody anti-rabbit iba1 (cat. no. 019–19741; Fujifilm) diluted 1:1000 in (1 % BSA, in 0.1 % TritonX-100 in 1 X PBS) was placed onto slides in the humidity chamber for a 2 hr incubation. Slides were rinsed again with 3 X (15 min each rinse) washes. Slides were incubated with secondary antibody Alexa-fluor 488 nm wavelength (A11070; Invitrogen by Thermo Fisher Scientific) goat-anti-rabbit antibody diluted 1:2000 in 1 X PBS/0.1% Triton and incubated in the humidity chamber for 2 hrs, followed by a 3 × 15 min rinse. Tissue was stained for 10 mins with (4′,6-diamidino-2-phenylindole; Sigma-Aldrich Cat. No. D9542) DAPI for nuclei visualization. Slides were rinsed with 3 × 15 min washes. Slides were mounted with Fluoromount G (Cat. No. 00-4958-02; Invitrogen by Thermo

Fisher Scientific) on coverslips (Cat. No. 48393-106; VWR) and imaged on a fluorescence microscope at 10 X and 60 X objectives (Nikon A1R Confocal & Super Resolution System, Nikon, Tokyo, Japan).

2.7. Enzyme-linked immunosorbent assay (ELISA)

Protein isolation from harvested murine brains from both the cerebral cortex and hippocampus was performed using T-PER® Tissue Protein Extraction Reagent (Cat. No. 78510, Thermo Fisher Scientific, Waltham, MA) with Halt™ Protease Inhibitor Cocktail (Cat. No. 87785, Thermo Fisher Scientific, Waltham, MA). Tissue lysates were diluted in ELISA sample buffer and S-adenosylmethionine (SAM) levels were detected using the SAM specific ELISA from Cell Biologics (cat. no STA-672). SAM levels were detected in tissue lysates of both the cerebral cortex and hippocampus via FLUOstar Omega (BMG Labtech; S/N: 415–2374) and adhered to protocols provided by the manufacturer.

2.8. In vitro cell culture

HT22 mouse hippocampal neuronal cell line was purchased from Millipore Sigma (SKU SCC129). For our *in vitro* experiments we cultured HT22 cells in supplemented DMEM (cat. no. 11320-033; Gibco) media with 10 % FBS, 1 % penicillin/streptomycin (cat. no. 15140122; ThermoFisher Scientific) and glutaMAX (cat. no. 35050079; Gibco). Cells were seeded at 30,000 cell density into 6-well plates until 70 % confluency. The cells were then treated with PF-9366 (cat. no. 30872; Cayman Chemicals) allosteric drug inhibitor (MAT2A inhibitor) at 25 μM (Wang et al., 2021) in 0.43 % DMSO for 24 hrs. Upon completion of experimentation, cells were washed twice with ice-cold 1X PBS over ice and lysed with 100 μl of RIPA lysis and extraction buffer (cat no. 89900; ThermoFisher Scientific) and protease cocktail inhibitor (cat. no. 78429; ThermoFisher Scientific) with cell scrapers. Cell lysates were centrifuged at 10,000 × *g* for 10 min at 4 °C. Supernatant was then removed for protein quantification and subsequent protein analysis.

2.9. Histology (Bielschowsky's Silver Stain Kit)

Mice were anesthetized and transcardially perfused with 1 X phosphate buffered saline (PBS, 20 ml, Cat. No. AAJ62036-K7, VWR, Radnor, PA), followed by 4 % paraformaldehyde (Cat. No. P6148, MilliporeSigma, Burlington, MA) in 0.1 mmol/L of PBS. The brains were removed and fixed in 4 % paraformaldehyde overnight at 4 °C immediately after perfusion. The brains were dehydrated in 30 % sucrose (Cat. No. S9378, MilliporeSigma, Burlington, MA) in 0.1 mmol/L PBS for 72 hrs at 4 °C before sectioning. The brains were sectioned into 30 μm slices on a sliding microtome with a −20 °C stage (Leica Biosystems, SM2000R) in NEG-50™ sectioning media (Cat. No. 6502, Thermo Fisher Scientific, Waltham, MA, USA), and placed on a 24-well dish in 1 X PBS before mounting them on adhesion slides (Cat. No. M1000W, StatLab, McKinney, TX). Once tissue sections were mounted on adhesion slides, the protocol was followed as indicated from Bielschowsky's silver stain kit (Abcam-ab245877). Slides were mounted with DPX mountant histology medium (06522-100 ML; Sigma) with coverslips (Cat. No. 48393-106; VWR) and visualized on a bright-field microscope at 4 X objective.

2.10. HPLC-MS/MS (neurotransmitter panel)

After each experimental endpoint, mice brains were harvested and dissected separating the cerebral cortex and hippocampus and stored at −80 °C for storage. Once all time points were completed, mouse cortex and hippocampus were weighed and annotated. An internal standard solution containing 6 isotope-labeled internal standards was used for 6 analytes in 70 % acetonitrile solution. Tissue samples were homogenized in the internal standard solution at 10 μl of 70 % acetonitrile solution per mg of tissue for 1 min, 3 X at 30 Hz with 2 metallic spheres to aid homogenization. Samples were injected and analyzed using an automated Q TRAP 6500 plus mass spectrometer equipped with a heated electrospray ionization source. LC separation was carried out on a C18 Ultra Performance Liquid Chromatography column for gradient elution. Neurotransmitter concentrations were quantified based on internal standards and expressed as nanomoles/gram (nmol/g).

2.11. Statistical analyses

A p value of <0.05 level of probability was considered significant. Results were expressed as means ± S.E.M. Statistical analysis were evaluated by student's t-test, paired-samples *t*-test, two-way ANOVA, and by one-way ANOVA (Tukey's *post-hoc* test) as appropriate with Graph-pad Prism v.8.0.2 (San Diego, CA).

3. Results

3.1. Repetitive and mild TBI (rmTBI) induced loss of consciousness in mice

Mice were exposed to 1 mild TBI hit (0.7 J) per day for 3 consecutive days (Fig. 1A) via the CHIMERA (Fig. 1B) and assessed for loss of righting reflex (LRR) (a measurement of loss of consciousness). Righting times in sham mice (anesthesia only) were (23.9 ± 5.63) (day 1), (28.3 ± 5.87) (day 2), and (36.8 ± 2.59) (day 3) in seconds. Righting times in rmTBI mice were (197 ± 42.6) (day 1), (158 ± 34.3) (day 2), and (161 ± 30.7) (day 3) in seconds. There was a statistical main effect [$F(1, 16) = 38.8$; $p < 0.0001$] between SHAM and rmTBI mice via two-way ANOVA with Tukey's *post-hoc* analysis to suggest rmTBI mice lost consciousness relative to their SHAM counterparts (Fig. 1C).

3.2. Iba1 was elevated in repetitive and mild traumatic brain injury

Ionized calcium binding adaptor molecule 1 (iba1), a microglia marker and indicator for inflammation was examined in the cortex and hippocampus via capillary electrophoresis and immunofluorescence in both SHAM and rmTBI mice. Our results suggest a significant elevation of iba1 protein expression in the hippocampus at both 3 (0.02 ± 0.001) arbitrary units (AU) and 7 (0.02 ± 0.001 AU) days post-rmTBI relative to SHAM (0.01 ± 0.001) (Fig. 2A). There were no significant changes of iba1 in the cortex, albeit the trend was similar to that of the hippocampus at 3 (0.020 ± 0.002 AU) and 7 (0.018 ± 0.004 AU) days post-rmTBI relative to SHAM (0.010 ± 0.002) (Fig. 2B). In addition, it has been previously shown that iba1 is increased and activated in the optic tract of rmTBI via the CHIMERA (Namjoshi et al., 2014); therefore, we probed for iba1 in the optic tract via immunofluorescence. We observed enhanced iba1 immunofluorescence in the optic tract to suggest increased

microglia number in rmTBI mice v. SHAM (Fig. 2C–N). Results are analyzed via one-way ANOVA with Tukey's *post-hoc* test.

3.3. Cytokine production was enhanced post repetitive and mild traumatic brain injury

Cytokine array was conducted to assess cytokine production in both the cortex and hippocampus in rmTBI. Our results suggest the following increase in cytokine production in the cortex: ICAM-1 was significantly elevated at 7 days (130 ± 13.5 pg/mL) post-rmTBI relative to SHAM (49.8 ± 6.82 pg/mL); IL-6 was also significantly increased at 1 (85.6 ± 13.4 pg/mL) and 3 (64.2 ± 7.98 pg/mL) days post-rmTBI relative to SHAM (0.88 ± 20.5 pg/mL); CD30L was significantly increased at 1 day (110 ± 39.0 pg/mL) relative to SHAM (14.4 ± 2.41 pg/mL); IL-5 was significantly increased at 1 day (138 ± 22.6 pg/mL) relative to SHAM (42.8 ± 4.83 pg/mL), followed by a significant decrease at 7 days (77.7 ± 16.1 pg/mL) relative to 3 days post-rmTBI (57.8 ± 9.91); IL-10 was significantly elevated at all time points 1 (449 ± 46.9 pg/mL), 3 (307 ± 27.7 pg/mL), and 7 (341 ± 37.3 pg/mL) days post-rmTBI relative to SHAM (167 ± 21.1 pg/mL). Results were analyzed via one-way ANOVA with Tukey's *post hoc* (Fig. 3A–E). In the hippocampus, there was a significant increase in the following cytokines: IL-1alpha at 1 day (8.6 ± 0.7 pg/mL) post-rmTBI relative to SHAM (5.1 ± 0.94 pg/mL); CD30L was significantly elevated at 1 day (48 ± 7.1 pg/mL) relative to SHAM (15 ± 1.4 pg/mL), followed by a significant decrease at 7 days (14 ± 3.4 pg/mL) relative to 1 day post-rmTBI; and IL-12p70 was significantly increased at 1 day (28 ± 3.1 pg/mL) relative to SHAM (17 ± 1.6 pg/mL). Results were analyzed via one-way ANOVA with Tukey's *post-hoc* analysis and SEM via descriptive statistics. Significant cytokine results were presented from the cortex and hippocampus (Fig. 3F–H).

3.4. PRMT7 cortical protein expression was decreased after repetitive and mild traumatic brain injury (rmTBI)

PRMT7 protein expression was examined in the cerebral cortex and hippocampus at 1, 3, and 7 days post-rmTBI. PRMT7 cortical protein expression was significantly decreased at 3 (0.58 ± 0.05) and 7 days (0.57 ± 0.03) as compared to sham (0.78 ± 0.03), but not at 1 day (0.78 ± 0.01) arbitrary units (AU) post-rmTBI via one-way ANOVA with Tukey's *post hoc* analysis (Fig. 4A). There were no significant changes in PRMT7 protein expression in the hippocampus at 1 (0.95 ± 0.04), 3 (0.91 ± 0.01), and 7 (0.90 ± 0.12) days post-rmTBI relative to sham (1.08 ± 0.08) (AU) (Fig. 4B). Lastly, there were no significant changes in PRMT7 mRNA expression in the cortex at 3 or 7 days post-rmTBI relative to SHAM as analyzed via one-way ANOVA with Tukey's *post hoc* analysis (Fig. 4C and D).

3.5. Monomethylarginine protein expression is decreased in the hippocampus after repetitive and mild traumatic brain injury (rmTBI)

MMA was analyzed to assess the catalytic function of PRMT7 post-rmTBI via capillary electrophoresis. Our results suggest no significant changes in the cerebral cortex (Fig. 5A) at any time points at 1 day (0.71 ± 0.09), 3 days (0.76 ± 0.09), and 7 days (0.62 ± 0.17) arbitrary units (AU) after rmTBI as compared to sham (0.56 ± 0.06). MMA was decreased in the hippocampus at 1 (1.07 ± 0.08), 3 (0.41 ± 0.07), and 7 days (1.71 ± 0.24) relative to SHAM (4.69 ± 0.83) (AU) post-rmTBI via one-way ANOVA with Tukey's *post-hoc* analysis (Fig. 5B).

3.6. S-adenosylmethionine levels are increased in the hippocampus post-rmTBI

The primary methyl donor, S-adenosylmethionine (SAM), was measured via ELISA both in the cortex and hippocampus of SHAM and rmTBI mice. In the cortex, SAM followed the same trend as the hippocampus, although not significant (Fig. 6A). SAM levels were significantly enhanced in the hippocampus at 3 days (1.20 ± 0.08 pg/mL) post-rmTBI relative to SHAM (0.83 ± 0.04 pg/mL), followed by a significant decrease at 7 days (0.88 ± 0.09 pg/mL) relative to 3 days post-rmTBI (Fig. 6B). Results were analyzed via one-way ANOVA with Tukey's *post-hoc* test.

3.7. MAT2B is enhanced in the hippocampus post-rmTBI

Methionine adenosyltransferase 2A/B (MAT2A and MAT2B) are responsible for producing S-adenosylmethionine (SAM; primary methyl donor for PRMT's), therefore we probed for MAT2A and MAT2B via capillary electrophoresis in our SHAM and rmTBI mice. Our results suggest a decrease of MAT2A protein expression in the hippocampus, although not significant at 7 days (0.81 ± 0.07 AU) ($p = 0.0562$) post rm-TBI relative to SHAM (0.96 ± 0.02 AU) (Fig. 7A). In addition, there was a significant elevation of MAT2B protein expression at 7 days (0.090 ± 0.007AU) relative to SHAM (0.071 ± 0.002AU) (Fig. 7B). Within the cerebral cortex there were no significant changes in MAT2B or MAT2A protein expression at 1, 3, or 7 days post-rmTBI (Fig. 7C and D). Results were analyzed via one-way ANOVA with Tukey's *post-hoc* test.

3.8. MAT2A inhibitor (PF-9366) reduced PRMT7 protein expression and activity

To determine if MAT2A inhibition can modulate PRMT7 protein expression and/or activity, we treated HT22 cells (mouse hippocampal cell line) with PF-9366 (allosteric MAT2A inhibitor at 25 μM for 24 h). Our results suggest that inhibition of MAT2A significantly decreased PRMT7 protein expression (1.30 ± 0.03 AU) relative to control (3.27 ± 0.05 AU) (Fig. 8A). In addition, MAT2A inhibition also reduced PRMT7 activity as indicated by a significant reduction of mono-methylarginine (1.87 ± 0.06 AU) relative to control (2.88 ± 0.040 AU) (Fig. 8B). Lastly, MAT2A inhibition also led to a significant increase in MAT2A protein expression (3.86 ± 0.06 AU) relative to control (1.59 ± 0.03 AU) and a decrease in MAT2B protein expression (0.18 ± 0.02 AU) relative to control (0.36 ± 0.01 AU) (Fig. 8C and D). Results were analyzed via student's t-test (Fig. 8A–D).

3.9. Repetitive and mild TBI (rmTBI) induced diffuse axonal injury

Diffuse axonal injury (DAI) was assessed qualitatively using Bielschowsky's Silver Stain Kit. Mouse histological coronal sections of SHAM, 1, 3, 7-days post-rmTBI were stained to assess the extent of DAI in our model of rmTBI mice. Our results indicate an increase in diffuse axonal injury as demonstrated by the darker brown staining as a result of increased silver deposition throughout the cerebral tissue post-injury (Fig. S1 A–D).

3.10. Glutamate is enhanced after mild and repetitive traumatic brain injury

We assessed glutamate levels in the cerebral cortex and hippocampus post-rmTBI via high-performance liquid chromatography mass spectrometry (HPLC-MS/MS). Our results suggest no significant changes in glutamate levels in the cerebral cortex at any of the time

points at 1 (6241 ± 75.27), 3 (6913 ± 489.9), or 7 days (5882 ± 568.5) as compared to SHAM (6466 ± 309.1) nanomole per gram (nmol/g) (Fig. S2 A). However, in the hippocampus, there was a significant increase 3 days (6714 ± 107.8) v. SHAM (5522 ± 235.3) with no changes at 1 (5777 ± 463.3) or 7 days (5780 ± 249.5) (nmol/g) post-rmTBI (Fig. S2 B). Results were analyzed via one-way ANOVA with Tukey's *post hoc* (Fig. S2 A–B).

3.11. BAX was elevated in mild and repetitive traumatic brain injury

Cell death was assessed post-rmTBI, via the apoptotic marker BAX and there were significant increases in BAX protein expression in the hippocampus 3 (0.03 ± 0.002) and 7 days (0.03 ± 0.002) v. sham (0.02 ± 0.003) (AU) post-rmTBI (Fig. S2 D). However, there were no significant changes in BAX protein expression in the cerebral cortex at any of the time-points, 3 (0.02 ± 0.001) or 7 days (0.02 ± 0.006) relative to sham (0.02 ± 0.003) arbitrary units (AU) (Fig. S2 C).

4. Discussion

Pathophysiological events of neuroinflammation, diffuse axonal injury, and excess glutamate were assessed to validate injury with previously published pre-clinical studies of TBI (Y. Li et al., 2020; Namjoshi et al., 2014; Santiago-Castaneda, Huerta de la Cruz, Martinez-Aguirre, Orozco-Santiago-Castaneda et al., 2022). In addition to these pathological findings, PRMT7 protein expression was significantly decreased in the cerebral cortex at 3 and 7 days post-rmTBI and MMA production was significantly decreased at 1, 3, and 7 days post-rmTBI in the hippocampus suggesting a significant reduction in PRMT7 activity. These changes in PRMT7 protein expression and activity correlated with the pathological findings of neuroinflammation as denoted by enhanced cytokine production in both the cortex and hippocampus as well as enhanced iba1 protein levels and microglia via immunofluorescence. The optic tract was specifically assessed as it has been one of the most consistent pathological findings across CHIMERA TBI users (McNamara et al., 2020).

PRMT7 dysfunction has been implicated in neurological activity via methylation of hyperpolarization-activated cyclic nucleotide-gated channels and sodium leak channels, affecting the neurotransmission within pyramidal cells of mice hippocampi as well as contribute to enhanced neuronal excitability via methylation of Nav1.9 channels within nociceptors contributing to hypersensitivity in transgenic mice (Ma et al., 2022); indicating PRMT7's essential role in maintaining neuronal integrity (Lee et al., 2019, 2020). In addition, PRMT7 has recently been described to have unique optimal physiological microenvironments affecting its catalytic activity (Lowe and Clarke, 2022). Lowe and Clarke have described optimal activity of PRMT7 at alkaline pH, sub physiological temperature (below 37 °C), and at lower ionic strengths below that of most intracellular environments (Lowe and Clarke, 2022). TBI-induced brain injury typically causes a decrease in pH due to elevated lactate production, increased acidosis, inflammation, and enhanced metabolic activity (Timofeev et al., 2013) all of which largely impact brain temperature (Mrozek et al., 2012; Rzechorzek et al., 2022) and can ultimately lead to a disruption of PRMT7 activity *in vivo*. Specific molecular changes in the cortex and hippocampus were observed

in our rmTBI studies, which have also been reported from various pre-clinical brain injury studies (Tashlykov et al., 2007; Svirsky et al., 2020; Voelz et al., 2021; Baranovicova et al., 2021) Anatomical differences and vascular supply between the cortex and hippocampus are major contributors to the functional differences between brain regions (Johnson, 2023). The vascular density is a fraction of the cortex, rendering the hippocampus more susceptible to ischemia-related injury (Johnson, 2023; Shaw et al., 2021). These established anatomical and physiological differences could explain in part why we see different PRMT7 enzymatic activity between the cortex and hippocampus as well as protein expression. Moreover, PRMT7 has been described to be highly expressed in the hippocampus relative to other brain regions (Lee et al., 2019), further supporting why PRMT7 activity is observed to be more affected in the hippocampus than the cortex. Our data supports a decrease in PRMT7 activity in the hippocampus in response to injury as suggested by the significant decrease in MMA production post-injury. Taken together, our results suggest a novel role of PRMT7 that correlate with our pathophysiological findings in our model of rmTBI.

Concomitant dysregulation of upstream PRMT mediators, methionine adenosyltransferase (MAT2A/B) and S-adenosylmethionine (SAM) also correlated with neuroinflammatory events, diffuse axonal injury, and excess glutamate pathologies. Methionine adenosyltransferase 2 (MAT2A) is responsible for SAM production, which is the universal methyl donor in the body, whereas MAT2B is the regulatory unit and can act to inhibit MAT2A activity (C. Li et al., 2022). MAT2A and the methyl donor SAM are upstream mediators of PRMT activity (Kalev et al., 2021). Our *in vivo* data suggest a decrease in MAT2A protein expression 7 days post-rmTBI suggesting a decrease in activity as evidenced by decreased SAM production (downstream product) at 7 days post-rmTBI in the hippocampus. This decrease in upstream PRMT mediators and/or activity can ultimately lead to a subsequent decrease in PRMT methylation activity. Moreover, MAT2A and B can form a heterotetradimer, in which MAT2B is able to elicit its' regulatory properties and inhibit MAT2A activity (Nordgren et al., 2011; Quinlan et al., 2017). The upregulation of MAT2B protein expression at 7 days also suggests inhibition of MAT2A activity, which is supported by the decreased SAM production at 7 day relative to 3 days rmTBI in the hippocampus. Furthermore, previous studies have suggested that MAT2B also regulates MAT2A activity by making it more susceptible to feedback inhibition by SAM (LeGros et al., 1997) and can inhibit the catalytic activity of MAT2A when SAM or methionine levels are high causing a reduction in downstream product formation. A significant upregulation in SAM production was observed 3 days post-rmTBI within the hippocampus suggesting negative feedback inhibition of MAT2A. Moreover, enhanced SAM levels could be a compensatory response to the decrease in PRMT7's catalytic function as denoted by the time dependent decreases in MMA production at 1, 3, and 7 days post-rmTBI. SAM is described to have tight regulation physiologically as it is estimated to be the second most involved cofactor in cellular function outside of ATP (Ducker and Rabinowitz, 2017), further supporting the time-dependent changes of SAM production *in vivo.*

Using HT22 hippocampal neuronal cell line we wanted to determine a mechanistic link between PRMT7 and upstream mediators MAT2A/B *in vitro*. PRMTs utilize SAM as the methyl donor to methylate histone and non-histone proteins (Zhang et al., 2021). Previous studies suggest MAT2A inhibition led to downstream disturbance in PRMT5 activity by

significantly reducing SAM production (Kalev et al., 2021; Konteatis et al., 2021; Marjon et al., 2016). Here, we show MAT2A inhibition *in vitro* can also modulate PRMT7 protein expression and activity via the allosteric MAT2A inhibitor PF-9366. Our data suggest that MAT2A inhibition led to a decrease in PRMT7 protein expression as well as enzymatic activity indicated by decreased MMA production (Fig. 8A and B). Moreover, we observed compensatory effects of MAT2A protein expression upon inhibition, similar to previous studies reporting compensatory effects (Quinlan et al., 2017; Konteatis et al., 2021) of MAT2A (Fig. 8C). A cartoon schematic diagram illustrates the changes in PRMT7 and upstream mediators both *in vivo* and *in vitro* (Fig. 9A and B). To our knowledge, we are the first to report MAT2A inhibition caused a significant reduction of PRMT7 protein expression and activity *in vitro*, as well as to suggest a role for PRMT7 in the rmTBI pathology *in vivo*.

5. Conclusions

Collectively, our three-hit paradigm of rmTBI enhanced iba1 protein expression, cytokine production, and induced diffuse axonal injury, via CHIMERA. In addition, our rmTBI paradigm contributed to a significant increase in glutamate levels to suggest excitotoxicity 3 days post-rmTBI. These pathophysiological findings correlated with a decrease in PRMT7 levels and activity as seen by the significant decrease in PRMT7 protein expression and MMA production post-rmTBI. Furthermore, the upstream mediators of PRMT7, MAT2A and MAT2B, were dysregulated *in vivo*. Inhibition of MAT2A using HT22 hippocampal neuronal cell line caused significant reduction of PRMT7 protein expression and MMA production, to suggest a link between MAT2A and PRMT7 activity *in vitro*. Overall, our results suggest that PRMT7 plays a major role in our murine model of rmTBI and a mechanistic link between PRMT7 and the upstream mediator MAT2A upstream mediator.

Supplementary Material

Refer to Web version on PubMed Central for supplementary material.

Funding sources

Funding and support for this study are from the NIH/NINDS 5R01NS096225-05, 1R01NS126273-01, the AHA 22PRE903112, 22TPA970253, 19CDA3466032, 21CDA856826, and the Louisiana State University Research Council, the Joanna G. Magale Foundation.

Data availability

Data will be made available on request.

Abbreviations:

rmTBI	repetitive and mild traumatic brain injury
MAT2A/B	methionine adenosyltransferase 2 A/B
SAM	s-adenosylmethionine

PRMT	protein arginine methyltransferase
PRMT7	protein arginine methyltransferase 7
DAI	diffuse axonal injury
ADMA	asymmetric dimethylarginine
SDMA	symmetric dimethylarginine
MMA	mono-methylarginine
CHIMERA	closed head impact of engineered rotational acceleration
LRR	loss of righting reflex

References

Baranovicova E, Kalenska D, Grendar M, Lehotsky J, 2021. Metabolomic recovery as a result of ischemic preconditioning was more pronounced in Hippocampus than in cortex that appeared more sensitive to metabolomic blood components. Metabolites 11 (8). 10.3390/metabo11080516.

Bodnar CN, Roberts KN, Higgins EK, Bachstetter AD, 2019. A systematic review of closed head injury models of mild traumatic brain injury in mice and rats. J. Neurotrauma 36 (11), 1683–1706. 10.1089/neu.2018.6127. [PubMed: 30661454]

Cali E, Suri M, Scala M, Ferla MP, Alavi S, Faqeih EA, Maroofian R, 2022. Biallelic PRMT7 pathogenic variants are associated with a recognizable syndromic neurodevelopmental disorder with short stature, obesity, and craniofacial and digital abnormalities. Genet. Med 10.1016/j.gim.2022.09.016.

Couto ESA, Wu CY, Citadin CT, Clemons GA, Possoit HE, Grames MS, Lin HW, 2020. Protein arginine methyltransferases in cardiovascular and neuronal function. Mol. Neurobiol 57 (3), 1716–1732. 10.1007/s12035-019-01850-z. [PubMed: 31823198]

Couto ESA, Wu CY, Clemons GA, Acosta CH, Chen CT, Possoit HE, Lin HW, 2021. Protein arginine methyltransferase 8 modulates mitochondrial bioenergetics and neuroinflammation after hypoxic stress. J. Neurochem 159 (4), 742–761. 10.1111/jnc.15462. [PubMed: 34216036]

Dash PK, Hergenroeder GW, Jeter CB, Choi HA, Kobori N, Moore AN, 2016. Traumatic brain injury alters methionine metabolism: implications for pathophysiology. Front. Syst. Neurosci 10, 36. 10.3389/fnsys.2016.00036. [PubMed: 27199685]

Dewitt DS, Perez-Polo R, Hulsebosch CE, Dash PK, Robertson CS, 2013. Challenges in the development of rodent models of mild traumatic brain injury. J. Neurotrauma 30 (9), 688–701. 10.1089/neu.2012.2349. [PubMed: 23286417]

Drieu A, Lanquetin A, Prunotto P, Gulhan Z, Pedron S, Vegliante G, Ali C, 2022. Persistent neuroinflammation and behavioural deficits after single mild traumatic brain injury. J. Cerebr. Blood Flow Metabol 42 (12), 2216–2229. 10.1177/0271678X221119288.

Ducker GS, Rabinowitz JD, 2017. One-carbon metabolism in Health and disease. Cell Metabol. 25 (1), 27–42. 10.1016/j.cmet.2016.08.009.

Ginsburg J, Huff JS, 2022. Closed Head Trauma StatPearls. Treasure Island (FL).

Jain K, Clarke SG, 2019. PRMT7 as a unique member of the protein arginine methyltransferase family: a review. Arch. Biochem. Biophys 665, 36–45. 10.1016/j.abb.2019.02.014. [PubMed: 30802433]

Johnson AC, 2023. Hippocampal vascular supply and its role in vascular cognitive impairment. Stroke 54 (3), 673–685. 10.1161/STROKEAHA.122.038263. [PubMed: 36848422]

Kalev P, Hyer ML, Gross S, Konteatis Z, Chen CC, Fletcher M, Marjon K, 2021. MAT2A inhibition blocks the growth of MTAP-deleted cancer cells by reducing PRMT5-dependent mRNA splicing and inducing DNA damage. Cancer Cell 39 (2), 209–224. 10.1016/j.ccell.2020.12.010 e211. [PubMed: 33450196]

Kernohan KD, McBride A, Xi Y, Martin N, Schwartzentruber J, Dyment DA, Chitayat D, 2017. Loss of the arginine methyltranserase PRMT7 causes syndromic intellectual disability with microcephaly and brachydactyly. Clin. Genet 91 (5), 708–716.10.1111/cge.12884. [PubMed: 27718516]

Konteatis Z, Travins J, Gross S, Marjon K, Barnett A, Mandley E, Marks KM, 2021. Discovery of AG-270, a first-in-class oral MAT2A inhibitor for the treatment of tumors with homozygous MTAP deletion. J. Med. Chem 64 (8), 4430–4449. 10.1021/acs.jmedchem.OcO1895. [PubMed: 33829783]

Lee SY, Vuong TA, So HK, Kim HJ, Kim YB, Kang JS, Cho H, 2020. PRMT7 deficiency causes dysregulation of the HCN channels in the CA1 pyramidal cells and impairment of social behaviors. Exp. Mol. Med 52 (4), 604–614. 10.1038/s12276-020-0417-x. [PubMed: 32269286]

Lee SY, Vuong TA, Wen X, Jeong HJ, So HK, Kwon I, Cho H, 2019. Methylation determines the extracellular calcium sensitivity of the leak channel NALCN in hippocampal dentate granule cells. Exp. Mol. Med 51 (10), 1–14. 10.1038/s12276-019-0325-0.

LeGros HL Jr., Geller AM, Kotb M, 1997. Differential regulation of methionine adenosyltransferase in superantigen and mitogen stimulated human T lymphocytes. J. Biol. Chem 272 (25), 16040–16047. 10.1074/jbc.272.25.16040. [PubMed: 9188509]

Li C, Gui G, Zhang L, Qin A, Zhou C, Zha X, 2022. Overview of methionine adenosyltransferase 2A (MAT2A) as an anticancer target: structure, function, and inhibitors. J. Med. Chem 65 (14), 9531–9547. 10.1021/acs.jmedchem.2c00395. [PubMed: 35796517]

Li Y, Glotfelty EJ, Namdar I, Tweedie D, Olson L, Hoffer BJ, Greig NH, 2020. Neurotrophic and neuroprotective effects of a monomeric GLP-1/GIP/Gcg receptor triagonist in cellular and rodent models of mild traumatic brain injury. Exp. Neurol 324, 113113 10.1016/j.expneurol.2019.113113. [PubMed: 31730763]

Lowe TL, Clarke SG, 2022. Human protein arginine methyltransferases (PRMTs) can be optimally active under nonphysiological conditions. J. Biol. Chem 298 (9), 102290 10.1016/jjbc.2022.102290. [PubMed: 35868559]

Ma T, Li L, Chen R, Yang L, Sun H, Du S, Liu JY, 2022. Protein arginine methyltransferase 7 modulates neuronal excitability by interacting with NaV1.9. Pain 163 (4), 753–764. 10.1097/j.pain.0000000000002421. [PubMed: 34326297]

Maas AIR, Menon DK, Adelson PD, Andelic N, Bell MJ, Belli A, Investigators, ., 2017. Traumatic brain injury: integrated approaches to improve prevention, clinical care, and research. Lancet Neurol. 16 (12), 987–1048. 10.1016/S1474-4422(17)30371-X. [PubMed: 29122524]

Maldonado LY, Arsene D, Mato JM, Lu SC, 2018. Methionine adenosyltransferases in cancers: mechanisms of dysregulation and implications for therapy. Exp. Biol. Med 243 (2), 107–117. 10.1177/1535370217740860.

Marjon K, Cameron MJ, Quang P, Clasquin MF, Mandley E, Kunii K, Marks KM, 2016. MTAP deletions in cancer create vulnerability to targeting of the mat2a/PRMT5/RIOK1 Axis. Cell Rep. 15 (3), 574–587. 10.1016/j.celrep.2016.03.043. [PubMed: 27068473]

McKee AC, Daneshvar DH, 2015. The neuropathology of traumatic brain injury. Handb. Clin. Neurol 127, 45–66. 10.1016/B978-0-444-52892-6.00004-0. [PubMed: 25702209]

McNamara EH, Grillakis AA, Tucker LB, McCabe JT, 2020. The closed-head impact model of engineered rotational acceleration (CHIMERA) as an application for traumatic brain injury pre-clinical research: a status report. Exp. Neurol 333, 113409 10.1016/j.expneurol.2020.113409. [PubMed: 32692987]

Mrozek S, Vardon F, Geeraerts T, 2012. Brain temperature: physiology and pathophysiology after brain injury, 2012 Anesthesiol Res Pract, 989487. 10.1155/2012/989487.

Namjoshi DR, Cheng WH, McInnes KA, Martens KM, Carr M, Wilkinson A, Wellington CL, 2014. Merging pathology with biomechanics using CHIMERA (Closed-Head Impact Model of Engineered Rotational Acceleration): a novel, surgery-free model of traumatic brain injury. Mol. Neurodegener 9, 55. 10.1186/1750-1326-9-55. [PubMed: 25443413]

Narayan C, Kumar A, 2012. Constitutive over expression of IL-1beta, IL-6, NF-kappaB, and Stat3 is a potential cause of lung tumorgenesis in urethane (ethyl carbamate) induced Balb/c mice. J. Carcinog 11, 9. 10.4103/1477-3163.98965. [PubMed: 22919282]

Nordgren KK, Peng Y, Pelleymounter LL, Moon I, Abo R, Feng Q, Weinshilboum RM, 2011. Methionine adenosyltransferase 2A/2B and methylation: gene sequence variation and functional genomics. Drug Metab. Dispos 39 (11), 2135–2147. 10.1124/dmd.111.040857. [PubMed: 21813468]

Quinlan CL, Kaiser SE, Bolanos B, Nowlin D, Grantner R, Karlicek-Bryant S, Grant SK, 2017. Targeting S-adenosylmethionine biosynthesis with a novel allosteric inhibitor of Mat2A. Nat. Chem. Biol 13 (7), 785–792. 10.1038/nchembio.2384. [PubMed: 28553945]

Rodari G, Villa R, Porro M, Gangi S, Iascone M, Elli F, Giavoli C, 2022. Short stature in PRMT7 Mutations: first evidence of response to growth hormone treatment. Eur. J. Hum. Genet 10.1038/s41431-022-01220-9.

Rzechorzek NM, Thrippleton MJ, Chappell FM, Mair G, Ercole A, Cabeleira M, O'Neill JS, 2022. A daily temperature rhythm in the human brain predicts survival after brain injury. Brain 145 (6), 2031–2048. 10.1093/brain/awab466. [PubMed: 35691613]

Santiago-Castaneda C, Huerta de la Cruz S, Martinez-Aguirre C, Orozco-Suarez SA, Rocha L, 2022. Cannabidiol reduces short- and long-term high glutamate release after severe traumatic brain injury and improves functional recovery. Pharmaceutics 14 (8). 10.3390/pharmaceutics14081609.

Sauerbeck AD, Fanizzi C, Kim JH, Gangolli M, Bayly PV, Wellington CL, Kummer TT, 2018. modCHIMERA: a novel murine closed-head model of moderate traumatic brain injury. Sci. Rep 8 (1), 7677. 10.1038/s41598-018-25737-6. [PubMed: 29769541]

Schwulst SJ, Trahanas DM, Saber R, Perlman H, 2013. Traumatic brain injury-induced alterations in peripheral immunity. J. Trauma Acute Care Surg 75 (5), 780–788. 10.1097/TA.0b013e318299616a. [PubMed: 24158195]

Shaw K, Bell L, Boyd K, Grijseels DM, Clarke D, Bonnar O, Hall CN, 2021. Neurovascular coupling and oxygenation are decreased in hippocampus compared to neocortex because of microvascular differences. Nat. Commun 12 (1), 3190. 10.1038/s41467-021-23508-y. [PubMed: 34045465]

Svirsky S, Henchir J, Li Y, Ma X, Carlson S, Dixon CE, 2020. Neurogranin protein expression is reduced after controlled cortical impact in rats. J. Neurotrauma 37 (7), 939–949. 10.1089/neu.2019.6759. [PubMed: 31691647]

Tashlykov V, Katz Y, Gazit V, Zohar O, Schreiber S, Pick CG, 2007. Apoptotic changes in the cortex and hippocampus following minimal brain trauma in mice. Brain Res. 1130 (1), 197–205. 10.1016/j.brainres.2006.10.032. [PubMed: 17174280]

Tasker RC, 2012. Spreading depolarisations and traumatic brain injury: time course and mechanisms. Lancet Neurol. 11 (5), 389–390. 10.1016/S1474-4422(12)70084-4, 389; author reply. [PubMed: 22516073]

Timofeev I, Nortje J, Al-Rawi PG, Hutchinson PJ, Gupta AK, 2013. Extracellular brain pH with or without hypoxia is a marker of profound metabolic derangement and increased mortality after traumatic brain injury. J. Cerebr. Blood Flow Metabol 33 (3), 422–427. 10.1038/jcbftn.2012.186.

Valenzuela I, Segura-Puimedon M, Rodriguez-Santiago B, Fernandez-Alvarez P, Vendrell T, Armengol L, Tizzano E, 2019. Further delineation of the phenotype caused by loss of function mutations in PRMT7. Eur. J. Med. Genet 62 (3), 182–185. 10.1016/j.ejmg.2018.07.007. [PubMed: 30006058]

Voelz C, Ebrahimy N, Zhao W, Habib P, Zendedel A, Pufe T, Slowik A, 2021. Transient focal cerebral ischemia leads to miRNA alterations in different brain regions, blood serum, liver, and spleen. Int. J. Mol. Sci 23 (1). 10.3390/ijms23010161.

Wang L, Hu B, Pan K, Chang J, Zhao X, Chen L, Yuan J, 2021. SYVN1-MTR4-MAT2A signaling Axis regulates methionine metabolism in glioma cells. Front. Cell Dev. Biol 9, 633259 10.3389/fcell.2021.633259. [PubMed: 33859984]

Xiong Y, Mahmood A, Chopp M, 2018. Current understanding of neuroinflammation after traumatic brain injury and cell-based therapeutic opportunities. Chin. J. Traumatol 21 (3), 137–151. 10.1016/j.cjtee.2018.02.003. [PubMed: 29764704]

Zhang F, Kerbl-Knapp J, Rodriguez Colman MJ, Meinitzer A, Macher T, Vujic N, Madl T, 2021. Global analysis of protein arginine methylation. Cell Rep Methods 1 (2), 100016. 10.1016/j.crmeth.2021.100016. [PubMed: 35475236]

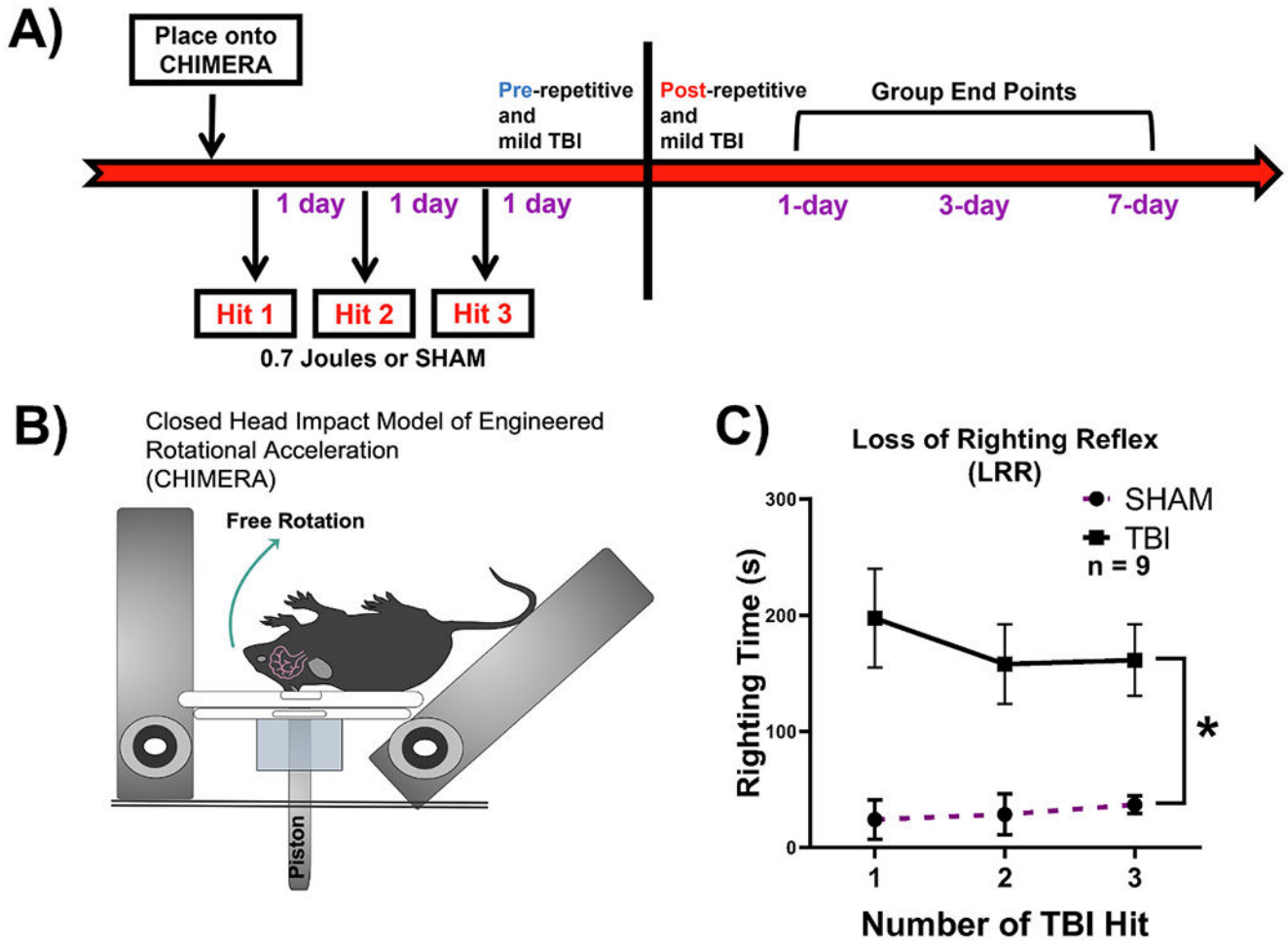

Fig. 1.

Loss of righting reflex (LRR) indicates loss of consciousness post-injury to validate repetitive and mild traumatic brain injury (rmTBI) in C57BL/6 male mice. (A) Cartoon of experimental design illustrating 3 repetitive hits separated by 24 h intervals at 0.7 J followed by assessment at 1, 3, and 7 days post-rmTBI. **(B)** We used a closed head impact model (CHIMERA) for the proposed TBI studies. The CHIMERA is a novel surgeiy-free model that allows for free rotation of the mouse brain to simulate real-world rotational and diffuse injury. **(C)** Loss of righting reflex was significantly increased in rmTBI (black line) mice as compared to age-matched (pink line) SHAM mice. Results were expressed as mean ± SEM. *$p \leq 0.05$ as compared to age-matched rmTBI mice, evaluated by two-way ANOVA with Tukey's post-hoc test.

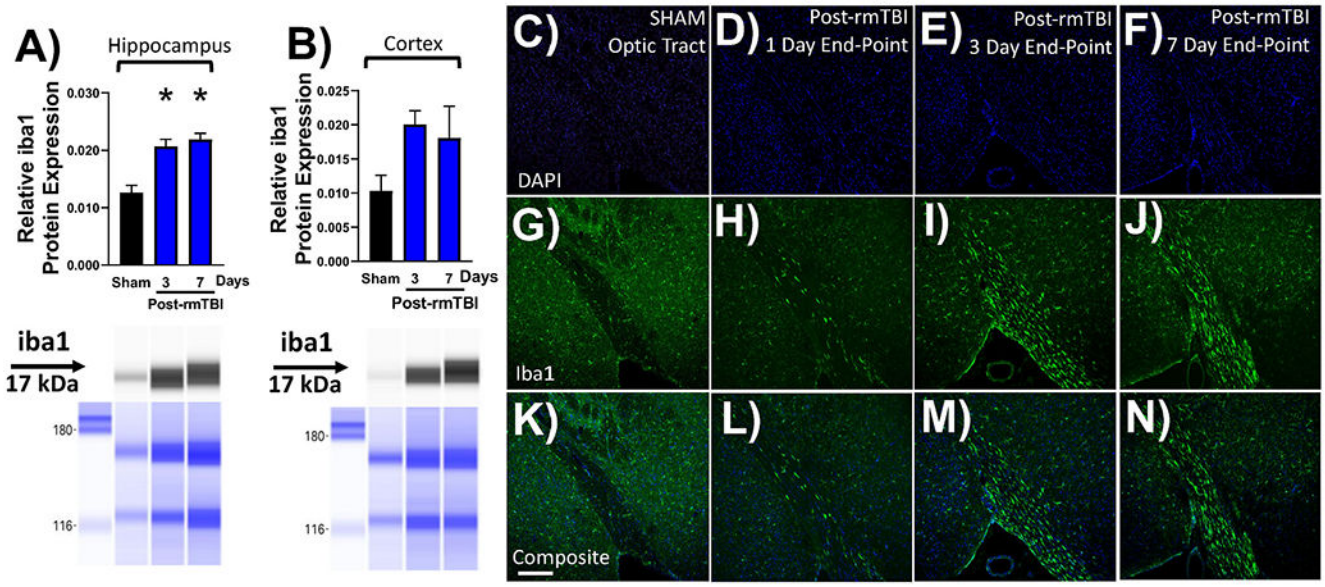

Fig. 2.

Repetitive and mild traumatic brain injury (rmTBI) enhanced iba1 protein expression in the hippocampus and optic tract. (A) Iba1 was enhanced in the hippocampus 3-day & 7 day post-rmTBI as compared to age-matched 8–12-week SHAM mice (black bar). **(B)** Iba1 was enhanced in the cortex but was not statistically significant. **(C–N)** Iba1 was assessed via immunofluorescence to demonstrate enhanced microglia within the optic tract at 1, 3, and 7 days post-rmTBI relative to SHAM mice. Results were expressed as mean ± SEM. *$p \leq 0.05$, as compared to age-matched rmTBI mice, evaluated by one-way ANOVA with Tukey's post-hoc test, (n = 3). Scale bar = 100 μm.

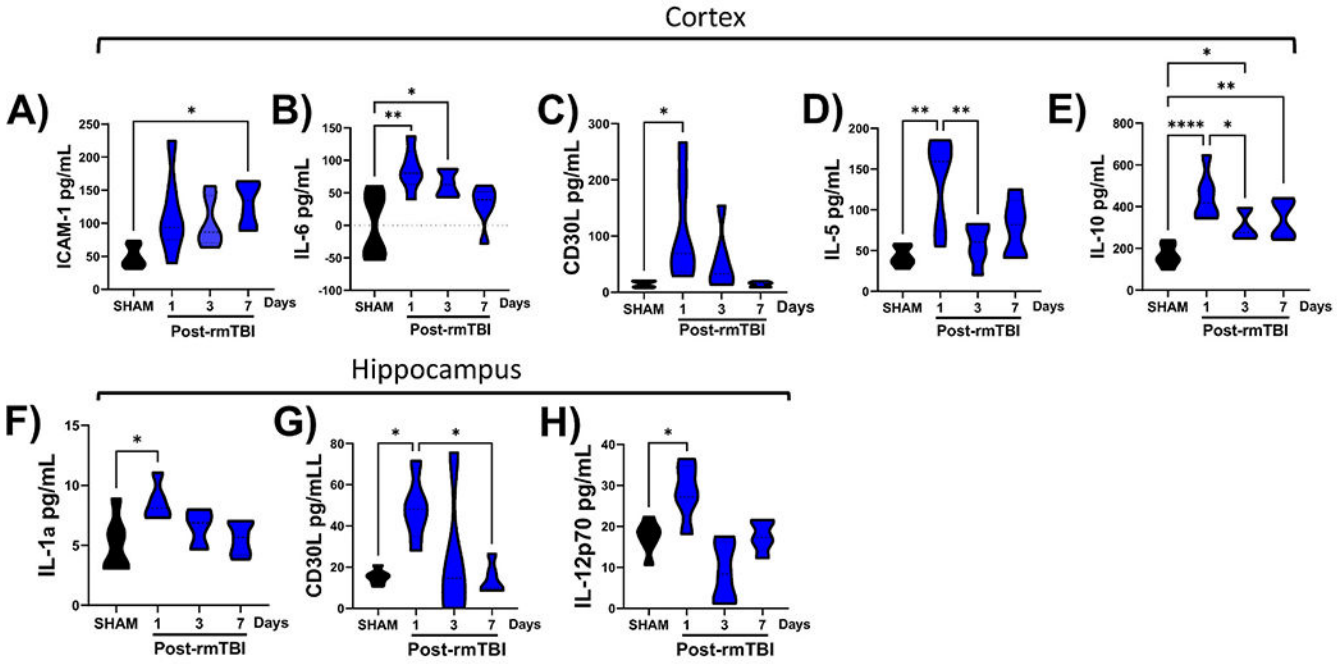

Fig. 3.

Repetitive and mild traumatic brain injuiy (rmTBI) induced cytokine production in the cortex and hippocampus. Cytokine array was performed in both the hippocampus and cortex of SHAM and rmTBI mice. **Cortex:** (**A)** ICAM-1 was significantly increased at 7 days post-rmTBI (blue violin) relative to sham (black violin). **(B)** IL-6 was significantly enhanced at 1 and 3 days post-rmTBI (blue violins) relative to SHAM (black violin). (**C)** CD30L was significantly elevated 1 day post-rmTBI (blue violin) relative to SHAM (black violin). (**D)** IL-5 was significantly elevated 1-day post-rmTBI relative to SHAM (black violin) and significantly decreased at 3 days relative to 1 day (blue violin) post-rmTBI. (**E)** IL-10 was significantly enhanced at all time points 1, 3, and 7 days post-rmTBI relative to SHAM (black violin). **Hippocampus: (F)** IL-1α was significantly enhanced at 1-day post-rmTBI (blue violin) relative to sham (black violin). (**G**) CD30L was significantly elevated at 1-day post-rmTBI (blue violin) relative to SHAM (black violin), followed by a significant decrease at 7 day relative to 1-day post-rmTBI. (**H)** IL-12p70 was significantly increased at 1-day post-rmTBI (blue bar) relative to SHAM (black violin). Violin polts represent the distribution of individual mice, and the middle dotted line represents the median; with the other two dotted lines representing quartiles. Results were expressed as *p ≤ 0.05, **p ≤ 0.01, ***p ≤ 0.001, ****p ≤ 0.0001 evaluated by one-way ANOVA with Tukey's post-hoc test with SEM descriptive statistics, (n = 3–6).

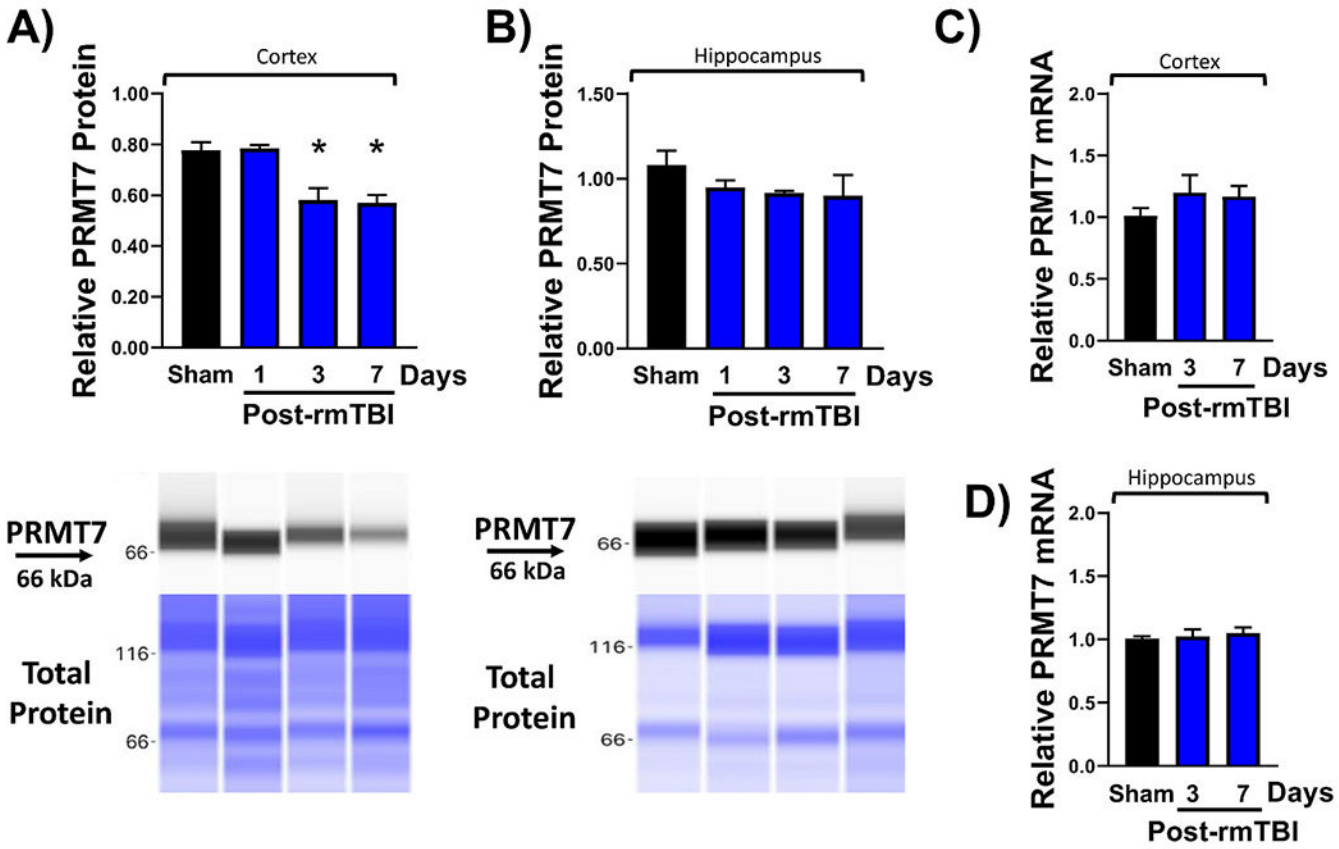

Fig. 4.

PRMT7 protein was altered in the cerebral cortex after repetitive and mild traumatic brain injury (rmTBI) (A) PRMT7 protein expression was significantly decreased in the **cortex** at 3 and 7 days (blue bar) relative to SHAM (black bar) and remain unchanged in the **(B) hippocampus** as compared to 8–12 weeks age-matched (black bar) SHAM mice. **(C)** PRMT7 mRNA levels remain unchanged at 3 and 7 days post-rmTBI in the **cortex** (blue bars) and **D)** unchanged at 3 and 7 days (blue bars) in the **hippocampus** post-rmTBI as compared to sham (black bar). Results were expressed as mean ± SEM. *$p \leq 0.05$, evaluated by one-way ANOVA with Tukey's post-hoc test, (n = 3–8).

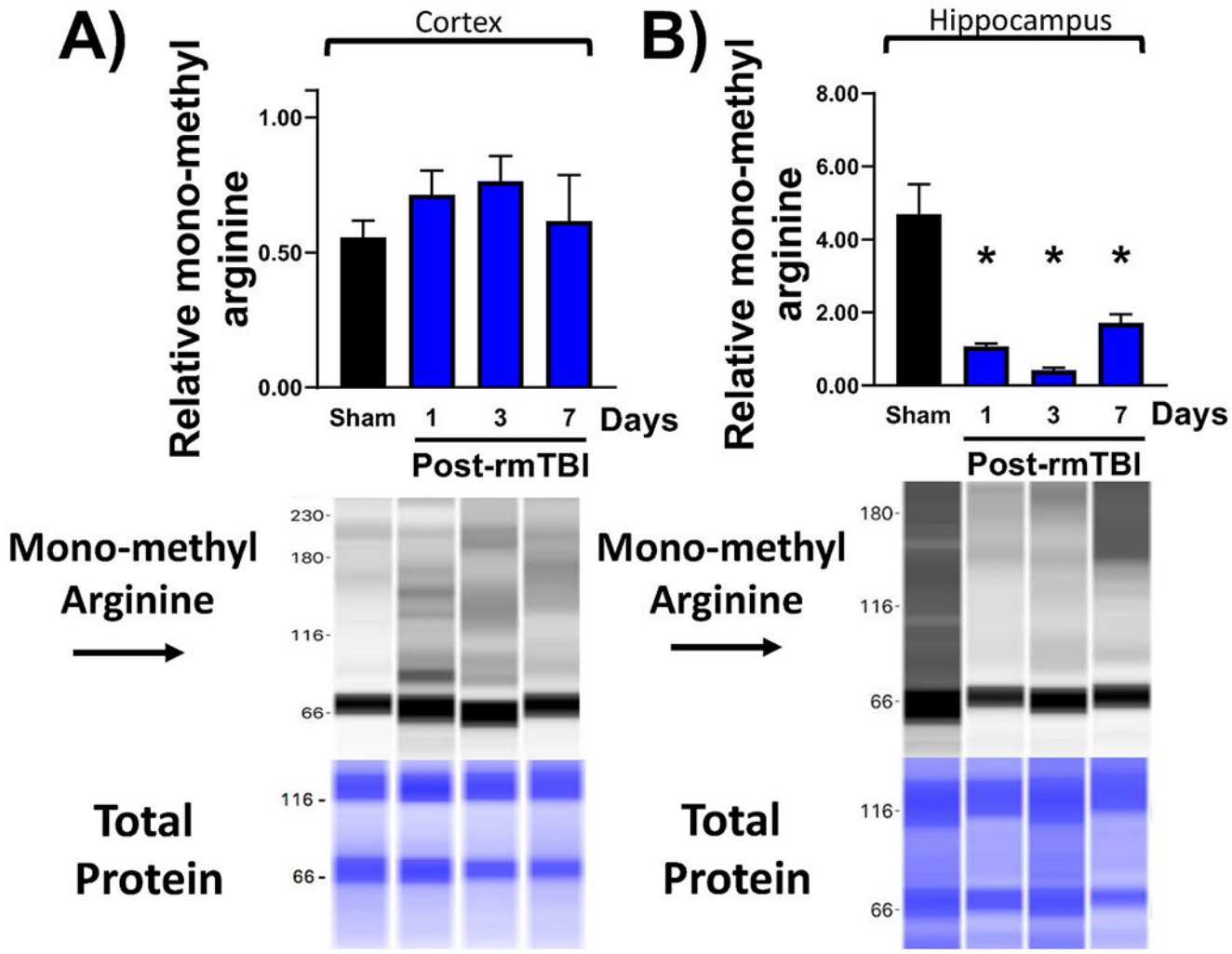

Fig. 5.

Monomethylarginine (MMA) production was decreased in the hippocampus after repetitive and mild traumatic brain injury (rmTBI). MMA, the catalytic end-product of PRMT7 was measured using capillary electrophoresis in the cortex and hippocampus. **(A)** MMA was unchanged in the **cortex** and significantly decreased in the **(B) hippocampus** (1, 3 and 7 day) as compared to SHAM mice (black bar). Results were expressed as mean ± SEM. *p ≤ 0.05, evaluated by one-way ANOVA with Tukey's post-hoc test, (n = 3–6).

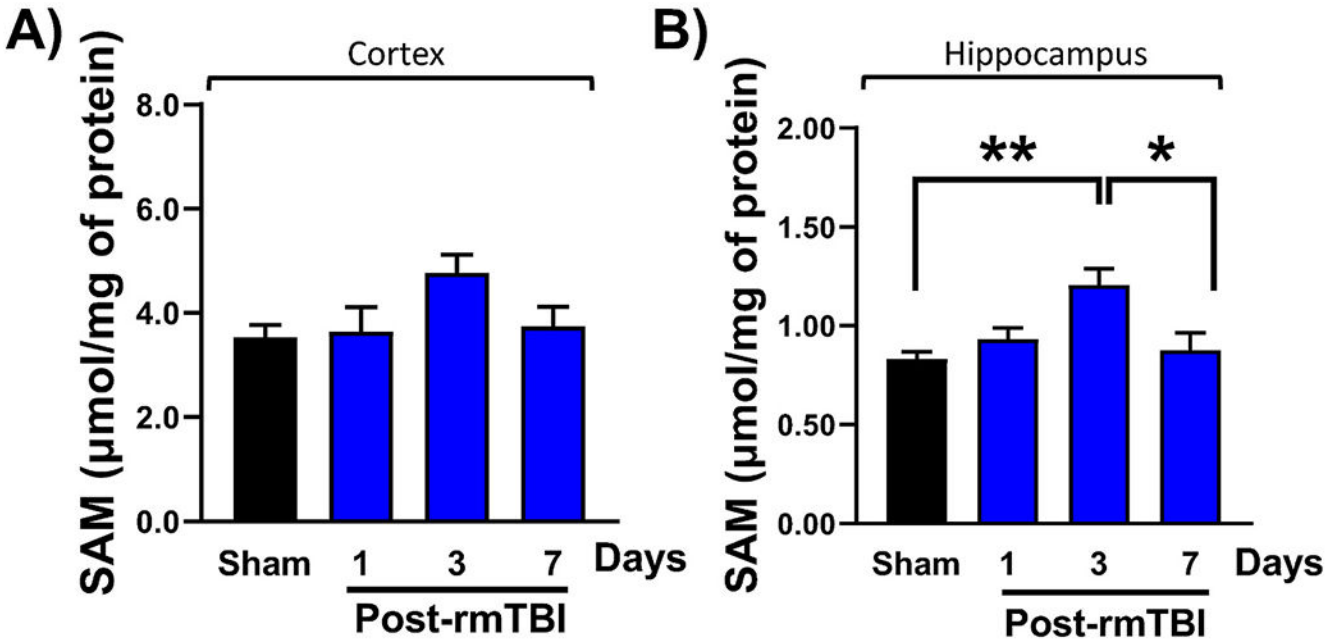

Fig. 6.

S-adenosylmethionine was increased 3 days post-rmTBI in the hippocampus after repetitive and mild traumatic brain injury (rmTBI). ELISA was performed to measure S-adenosylmethionine (SAM) levels in the cortex and hippocampus of mice tissue lysates. **(A)** There were no significant differences in SAM concentration in the **cortex**, however, the levels followed the same trend seen in the hippocampus. **(B)** There was a significant elevation of SAM levels within the **hippocampus** 3 days (blue bar) post-rmTBI relative to SHAM (black bar), followed by a significant decrease at 7 days (blue bar) relative to 3 days post-rmTBI. Results were expressed as mean ± SEM. *$p \leq 0.05$, **$p \leq 0.01$, evaluated by one-way ANOVA with Tukey's post-hoc test, ($n = 4–5$).

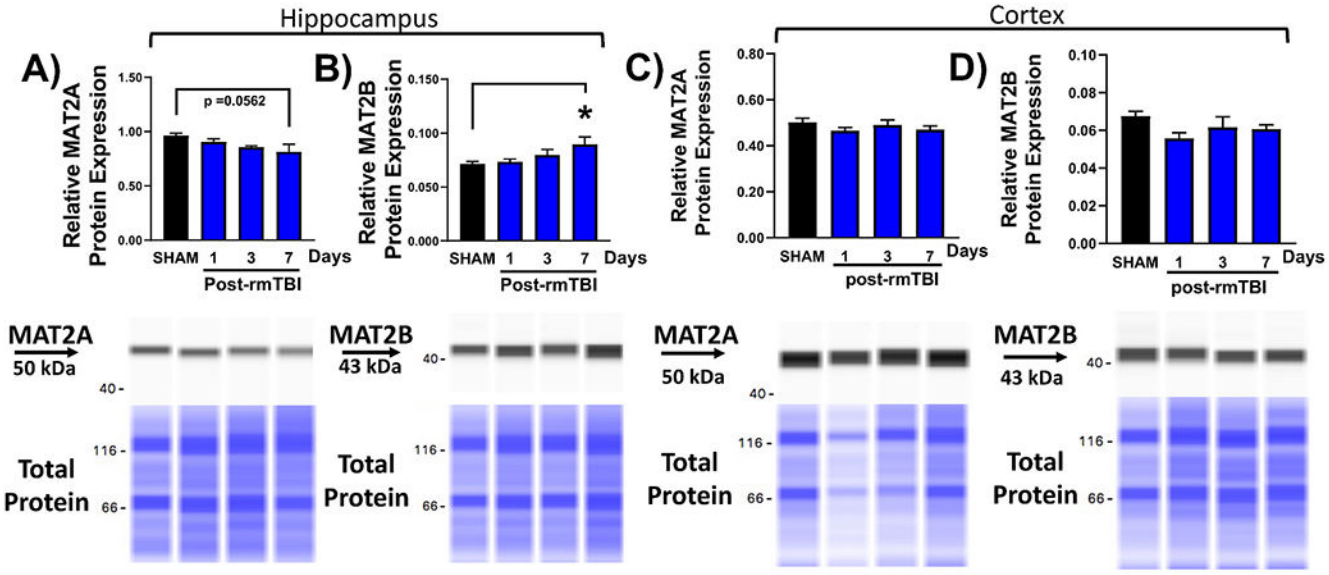

Fig. 7.

MAT2A was decreased and MAT2B was increased in the hippocampus post-rmTBI. MAT2A and MATB were assessed via capillary electrophoresis. **(A)** MAT2A (catalytic subunit) had a trending decrease at 7 days (blue bar) relative to SHAM (black bar). **(B)** MAT2B (regulatory subunit) was significantly enhanced 7 days (blue bar) post-rmTBI relative to SHAM (black bar). **(C–D)** MAT2A and MAT2B were unchanged in the cerebral cortex post-rmTBI. Results were expressed as mean ± SEM. *p ≤ 0.05, evaluated by one-way ANOVA with Tukey's post-hoc test, (n = 3–6).

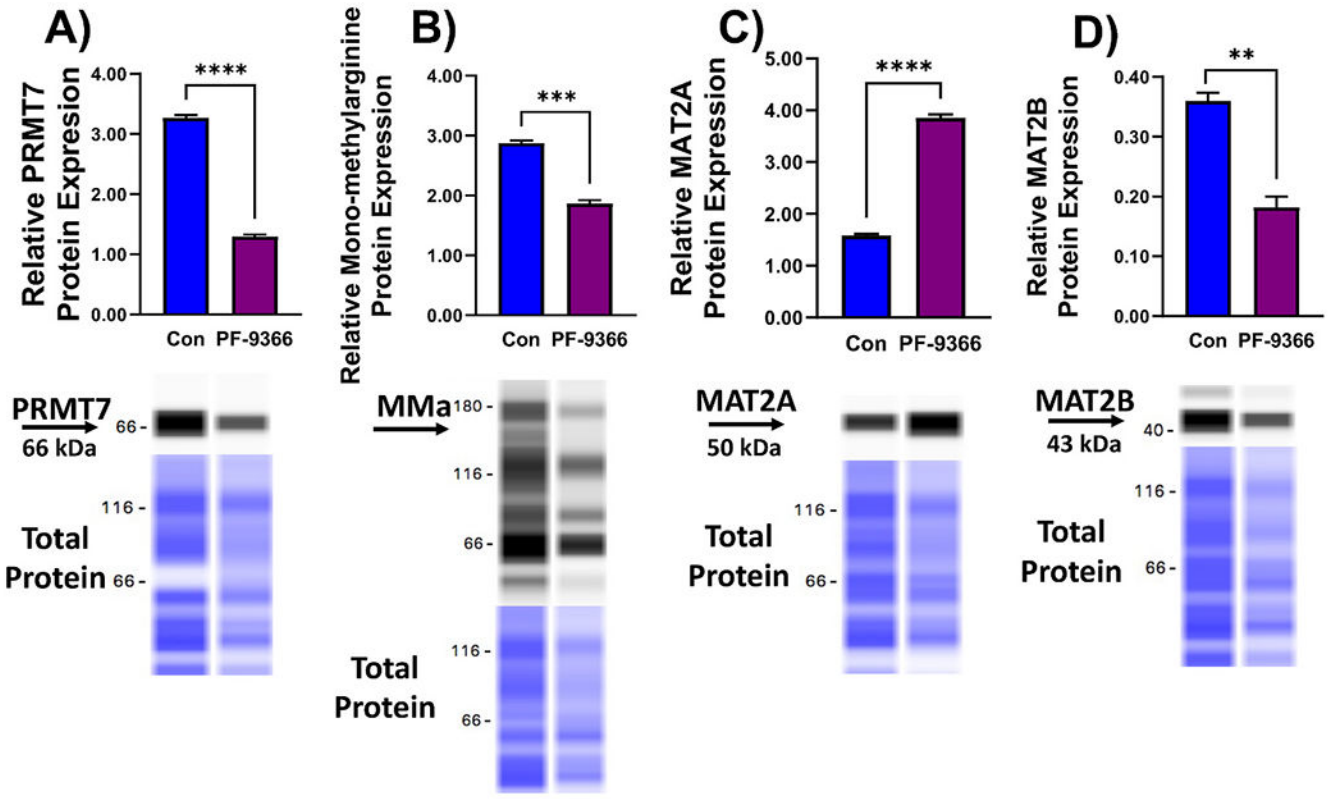

Fig. 8.

MAT2A inhibitor reduced PRMT7 protein expression and MMA production. PF-9366 allosteric inhibitor was used (25 μM) to inhibit MAT2A in HT22 cells for 24 hrs. Inhibition of MAT2A significantly decreased **(A)** PRMT7 protein expression **(B)** decreased mono-methylarginine (MMa) production **(C)** increased MAT2A protein expression and significantly decreased **(D)** MAT2B protein expression. Results were expressed as mean ± SEM. *p ≤ 0.05, **p ≤ 0.01, ***p ≤ 0.001, ****p ≤ 0.0001 evaluated by student's t-test. (n = 3).

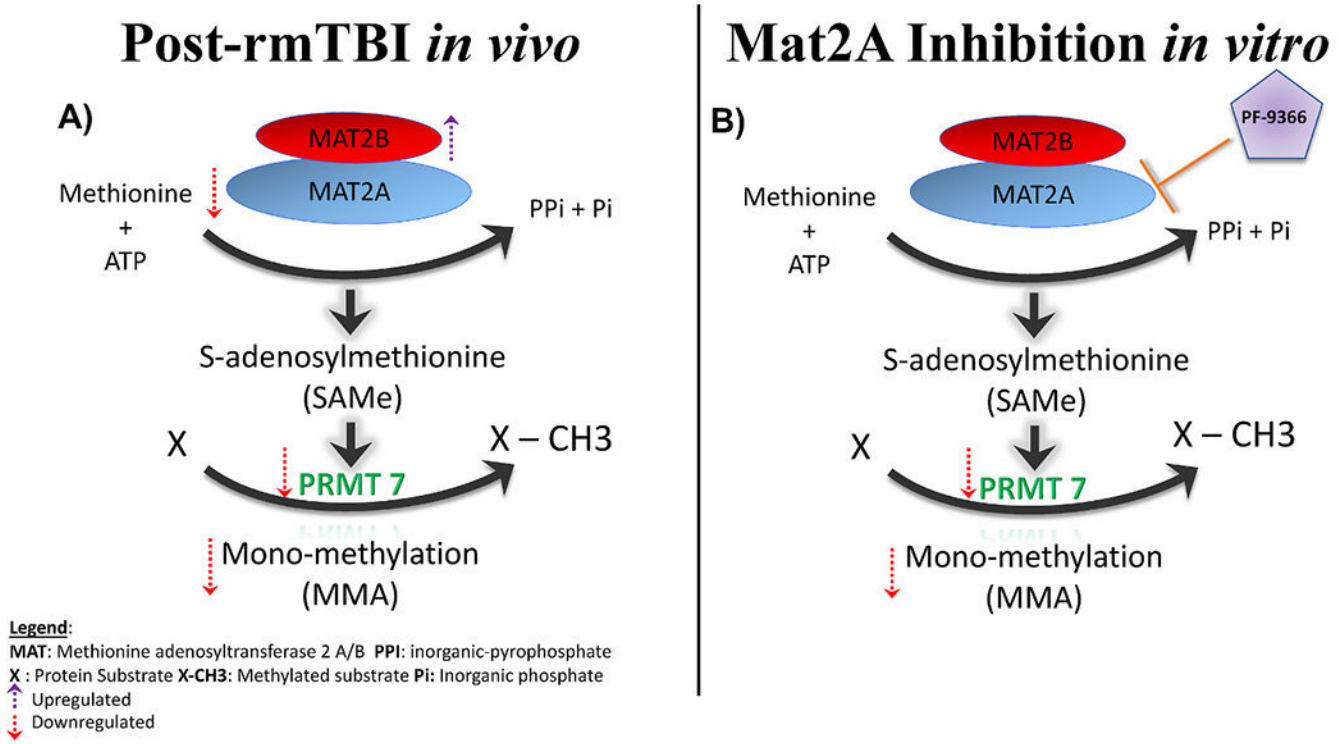

Fig. 9.

Schematic diagram of methionine-adenosyltransferase 2 A/B *in vivo*. **(A)** MAT2A is the catalytic subunit and MAT2B is the regulatory subunit and can associate to form a heterotetramer to synthesize s-adenosylmethionine (SAM) via methionine and ATP. Our *in vivo* studies of rmTBI reveal a dysregulation in the methionine metabolism that is potentially contributing to downstream disruption of PRMT7 protein expression and activity. Our results suggest PRMT7 protein expression and activity are downregulated post-rmTBI and could be attributed to the upstream dysregulation in methionine metabolism. **(B) Methionine-adenosyltransferase 2 A/B *in vitro*.** Our *in vitro* studies in HT22 cells using the MAT2A inhibitor (PF-9366) indicate that MAT2A inhibition affects not only PRMT7 protein expression, but activity as indicated by the significant decrease in mono-methylarginine (MMA, PRMT7 end-product). Purple arrows = upregulation, red arrows = down-regulation. These results suggest a possible mechanism of PRMT7 post-rmTBI.